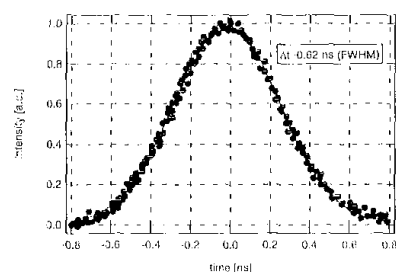
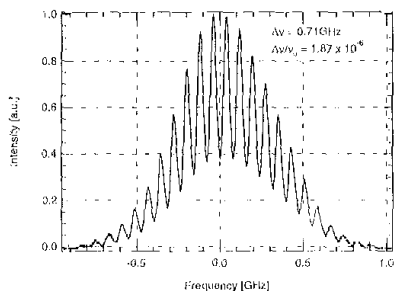


CThB2 Fig. 1. Schematic diagram of the system.



CThB2 Fig. 2. Temporal profile of the oscillator output.



CThB2 Fig. 3. Bandwidth of oscillator.

superior to the incoherent light for this purpose. The narrow-bandwidth harmonics are also useful for resonant core excitation of atoms and solids. Along this line, an all-solid-state, narrow-bandwidth, tunable, high-average-power Ti:sapphire laser has been developed.

This system consists of an oscillator, a regenerative amplifier, 4-pass amplifier and 1-pass amplifier (Fig. 1). An amplifier chain is almost equivalent to a 22-fs, 0.2-TW system.² Sub-nanosecond pulses do not need a stretcher and a compressor unlike a chirped pulse amplification system.

Sub-nanosecond pulses are generated in the oscillator. We modified a 100-ps "Tunami" (Spectra Physics), by inserting a 2-mm-thick solid etalon, resulting in a 0.62-ns pulse (FWHM) (Fig. 2).³ Figure 3 shows the spectrum measured at 800 nm by a scanning Fabry-Perot spectrum analyzer (SP-800 Burleigh Inst. Inc.). The 0.71-GHz (FWHM) bandwidth gives the time-bandwidth product

of 0.44, which is near the transform limit for a Gaussian pulse.

All Ti:sapphire crystals in the amplifier chain in this system are pumped by intracavity, frequency doubled, diode-pump, Q-switched Nd:YAG lasers (MITSUBISHI ELECTRIC CORP. MEL-Green100). Two green lasers are operated at 5 kHz with output powers of 56 W and 83 W respectively. The former is used for pumping the regenerative amplifier and the 4-pass amplifier while the latter is for a final 1-pass amplifier.

A 37-W output power is obtained with a 4-mm-diameter beam profile. This system is tunable from 750 nm to 850 nm without changing the present mirror set, although the range can be extended with a different mirror set. A 15.6-W SHG power is obtained from a 5-mm-log BBO type I crystal by focusing the output beam with a 1-m focal length lens. The harmonics in the VUV and XUV will be generated by resonant 4-wave and 6-wave mixing of ω , 2ω , 3ω in rare gases by using the tunability of the fundamental pulse.

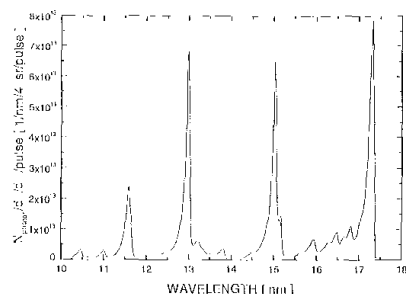
1. T. Sato, T. Yokkoya, Y. Naitoh, T. Takahashi, K. Yamada, Y. Endoh, "Pseudogap of Optimally Doped $\text{La}_{1.85}\text{Sr}_{0.15}\text{CuO}_4$ Observed by Ultrahigh-Resolution Photoemission Spectroscopy," *Phys. Rev. Lett.* **83**, 2254-2257 (1999).
2. Y. Nabekawa, T. Togashi, T. Sekikawa, S. Watanabe, S. Konno, T. Kojima, S. Fujikawa, K. Yasui, "All-solid-state 10kHz high-Peak-power Ti:sapphire laser system," *Ultrafast Optics 1999 MOA*, 21-23 (1999).
3. M. Watanabe, R. Ohmukai, K. Hayasaka, H. Imajo, S. Urabe, "High-power second-harmonic generation with picosecond and hundreds-of-picosecond pulses of a cw mode-locked Ti:sapphire laser," *Opt. Lett.* **19**, 637-639 (1994).

CThB3 8:30 am

The droplet laser plasma source for EUV lithography

G. Schriever, M. Richardson, E. Turcu,* *School of Optics & CREOL, Univ. of Central Florida, 4000 Central Florida Blvd., Orlando, Florida 32816-2700, USA; E-mail: mcr@creol.ucf.edu*

Extreme ultraviolet lithography (EUVL) is now considered the leading technology to replace optical lithography at the 100-nm node for the production of advanced computer chips later this decade.¹ EUVL is based on the use of all-reflective astigmatic multilayer-coated optics at 13 or 11 nm and a reflective 5:1 reduction mask illuminated by a bright point source.² Currently the source of choice is a high repetition-rate (>1kHz) laser-plasma, that must provide at least 7 W of radiation within a 3% spectral bandwidth, and be sufficiently free of particulate debris to ensure the long-time life of multilayer collimating optics.^{2,3} Two laser-plasma source approaches are presently being pursued, one based on a high-pressure Xenon gas jet target,³ and the other on plasmas produced from microscopic water droplets.^{5,6} The water droplet laser



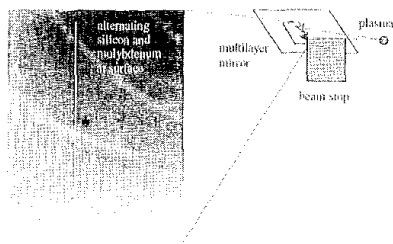
CThB3 Fig. 1. Calibrated spectral emission of the water droplet laser plasma EUV source.

plasma was introduced in 1993,^{5,6} as a bright source of 13-nm and 11.6-nm line emission from lithium-like oxygen,⁷ generated by 10-ns duration, Nd:YAG laser pulses at $\sim 10^{12}$ W/cm². These mass-limited targets are expected to be totally ionized, avoiding completely the particulate target debris that plagued earlier sources.⁸ Our previous work with a 100-kHz droplet system and a 10-Hz laser demonstrated the attractive features of this approach.⁹

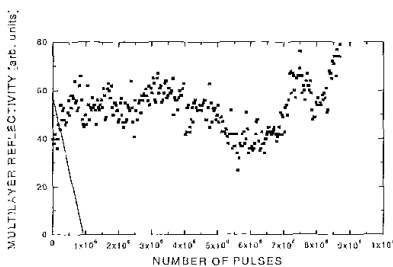
We now present a detailed quantitative study of this source, performed with a 100-Hz laser, that characterizes the radiation efficiency and the long-term operation. The results show that the droplet laser plasma source comes close to satisfying all the near-term needs of EUVL. In particular we demonstrate an overall conversion efficiency of laser light to 13-nm emission within the required spectral bandwidth in excess of 0.6%, comparable to any other existing source at this wavelength. In addition we have performed an exhaustive examination of the long-term effects of plasma emissions on the reflectivity of multilayer mirrors, exposed to this source. This included detailed surface science studies of the multilayer mirrors after EUV radiation doses approaching those anticipated in a first generation exposure tool. This study has led to the development of novel techniques that extend debris-free operation of this source by over an order of magnitude to close to that needed for long-term, continuous use, [10¹⁰ shots], at 1 kHz.

These experimental tests were performed with a commercial Q-switched Nd:YAG laser, emitting 10-ns laser pulses of ~ 250 -mJ energy focused to an un-optimized beam profile of ~ 25 -m diameter, coincident and synchronized to a 100-kHz train of 40-m diameter water droplet. Hydrodynamic code calculations estimate the ~ 30 -eV plasma created is completely ionized, producing a predominance of excited lithium-like oxygen ions that emit the recombination emission shown in Fig. 1. The narrow 13-nm line, produced with an efficiency of 0.63%, provides some advantages for EUVL over the broadband emission from other targets. Further studies on optimizing the emission at the two wavelengths will be reported.

Studies of the long-term effects of plasma emissions on multilayer mirrors are performed with Mo/Si surrogate mirrors placed some 32 nm from the target, accepting a single-shot fluence some 50 times greater than



CThB3 Fig. 2. Electron micrograph of 13-nm multilayer mirror exposed to long-term ion emission from the target.



CThB3 Fig. 3. Impact of the incorporation of an ion repeller field on the multilayer reflectivity lifetime. The straight line represents the lifetime without the repeller field.

that expected for the first mirror in an EUVI system. They reveal a number of interesting phenomena not previously observed in EUVI laser plasma investigations. These include the progressive sputtering of Mo and Si layers from multilayer mirrors after $>10^6$ shots, identified by electron microscopy, (Fig. 2.) and the consequential reduction in the reflectivity of the mirror, shown by the solid line in Fig. 3. These effects might put a limitation of $\sim 10^8$ shots on the lifetime of an EUVI mirror. To avoid this limitation we are investigating several avenues. For instance, the application of a repeller field between the target and the mirror has a dramatic effect on the mirror reflectivity lifetime, Figure 3., showing that the surrogate mirror reflectivity survives more than 10^7 shots. These tests, together with detailed materials characterization of the mirror surface, and ongoing further experiments provide optimism that the effective lifetime can be extended beyond 10^9 shots.

*JMAR Res. Inc., USA

1. Proc. 1998 International Sematech Mtg.
2. C.W. Gwyn, R. Stulen, D. Sweeney, D. Attwood, *J. Vac. Sci. Technol. B* **16**, 3 (1998).
3. A.M. Hawryluk, N.M. Ceglio, *Appl. Optics* **32**, 7062-7067 (1993).
4. G.D. Kubiak, I.J. Bernardez, K. Krenz, D. O'Connell, R. Gutowski, A. Todd, *TOPS*, IV, 66, (1996).
5. M. Richardson, K. Gabel, F. Jin, W.T. Silfvast, *Proc. OSA Top. Mtg. Soft x-ray Projection Lithography*, OSA, Washington DC, Vol. 18, pp. 156-162, (1993).
6. L. Rymell, H. Hertz, *Opt. Comm.* **103**, 105 (1993).
7. F. Jin, M. Richardson, *Appl. Opt.* **34**, 5750 (1995).

8. W.T. Silfvast, M.C. Richardson, H.A. Bender, A. Hanzo, V. Yanovsky, F. Jin, J. Thorpe, *J. Vac Science & Tech B* **10**, 3126 (1992).
9. M. Richardson, D. Torres, C. DePriest, F. Jin, G. Shimkaveg, *Opt Comm.* **145**, 109 (1998).

CThB4 9:00 am

Generation of diffraction-limited femtosecond beams using spatially-multimode nanosecond pump sources in parametric chirped pulse amplification systems

A. Galvanuskas, A. Hariharan, F. Raksi, K.K. Wong, D. Harter, G. Imeshev, M.M. Fejer, *IMRA America, Inc., 1044 Woodridge Ave., Ann Arbor, Michigan 48105, USA; E-mail: albnisg@imra.com

Currently, a number of important practical applications of ultrashort high-energy pulses are emerging, and, as a consequence, a need arises to significantly improve compactness and reliability of high-energy ultrafast sources. Optical fiber lasers and amplifiers offer a particularly promising avenue of the technological development in this direction, due to the robustness, reliability and the potential for component-integration, which is characteristic to fiber optics. The main obstacle, however, is the traditional limitation on the peak powers achievable in optical fibers due to the restricted size of a single-mode core.

Here we demonstrate that this limitation

can be bypassed by using multimode large-core fibers in conjunction with parametric chirped pulse amplification (PCPA). PCPA recently emerged as a practical technique providing efficient and simple nanosecond-pulse to femtosecond-pulse energy conversion through a high single-pass gain in a three-wave quasi-phase-matched parametric amplifier.^{1,2}

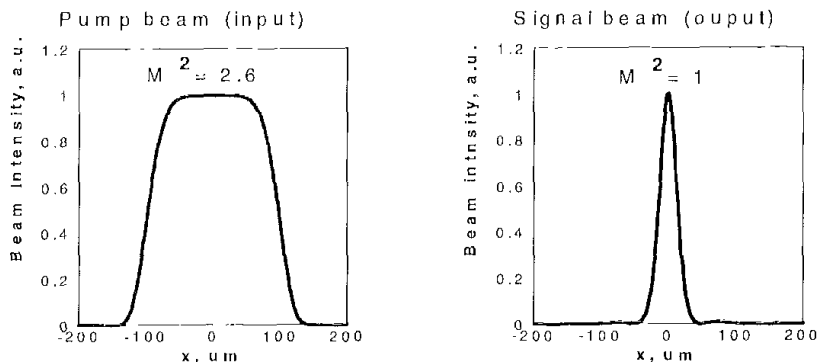
It is well established that stable two-transverse-dimensional spatial solitons can exist in frequency doubling crystals. Because such solitons emerge due to $\chi^{(2)}$ nonlinearity, they are known as quadratic solitons and are stable cylindrically symmetric solutions of the coupled-mode equations describing the SHG process at some phase-mismatch conditions.³ Furthermore, at phase-matching conditions stable spatial solitary waves can exist due to $\chi^{(2)}$ nonlinearity.⁴ Here we exploit the fact that such solitary waves also develop in the three-wave optical parametric interaction, which can be described by a standard set of three coupled-wave equations:

$$\frac{\partial E_1}{\partial z} + \frac{i}{2k_1} \nabla_{\perp}^2 E_1 = i\kappa_1 E_3 E_2^* \exp i\Delta kz$$

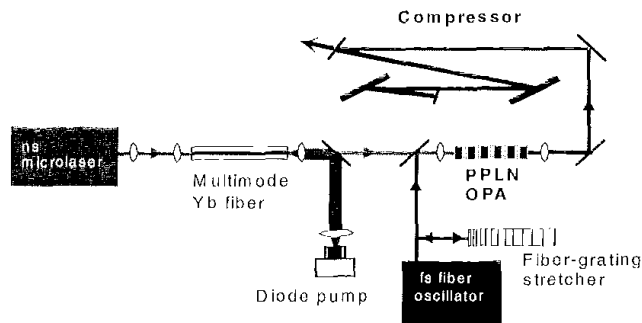
$$\frac{\partial E_2}{\partial z} + \frac{i}{2k_2} \nabla_{\perp}^2 E_2 = i\kappa_2 E_3 E_1^* \exp i\Delta kz$$

$$\frac{\partial E_3}{\partial z} + \frac{i}{2k_3} \nabla_{\perp}^2 E_3 = i\kappa_3 E_1 E_2 \exp i\Delta kz$$

Here $i = 1, 2, 3$ refers to the signal, idler and pump beams respectively. These equations fully describe spatial mode evolution in a real parametric amplifier by including effects of



CThB4 Fig. 1. Calculated far-field profiles of non-diffraction-limited pump beam at the input and diffraction-limited signal beam at the output of a parametric amplifier.



CThB4 Fig. 2. Multimode-fiber based PCPA system.